Clinical & Experimental Ophthalmology

WILEY

Clinical & Experimental Ophthalmology

ORIGINAL ARTICLE-CLINICAL SCIENCE OPEN ACCESS

Femtosecond Laser Created Corneal Allogenic Intrastromal Ring Segments for Keratoconus

David J. Gunn | Rebecca A. Cox | Brendan Cronin

Queensland Eye Institute, Brisbane, Queensland, Australia

Correspondence: Rebecca A. Cox (rebecca.cox@qei.org.au)

Received: 30 March 2025 | **Revised:** 18 February 2026 | **Accepted:** 1 March 2026

Keywords: allogenic transplantation | cornea | keratoconus

ABSTRACT

Background: To evaluate the clinical outcomes of femtosecond laser-created corneal allogenic intrastromal ring segments (femto-CAIRS) in keratoconic eyes using a newly described nomogram.

Methods: This retrospective case series recruited 85 eyes from 75 patients. Corrected and uncorrected visual acuity (CDVA/UDVA), refractive error, corneal topography, and higher-order aberrations were measured prior to surgery and ≥ 3 months post-operatively. All CAIRS were created using a femtosecond laser and the Brisbane nomogram was used to determine segment width, thickness, arc length, implantation axis and channel depth based on individual corneal topography.

Results: The mean follow-up time was 7.5 ± 5.0 months; 18 eyes had prior cross-linking (CXL), 30 underwent simultaneous CXL, and 37 had no CXL. Postoperatively, UDVA improved by 0.4 logMAR ($p < 0.001$) and CDVA by 0.2 logMAR ($p < 0.001$). There was an improvement of 5 or more lines in 31 eyes (43.7%), 8 eyes (11.3%) had no change in UDVA, 1 eye lost 1 line, and 1 eye lost 2 lines. There was a significant reduction in the mean spherical equivalent, refractive astigmatism, flat K, steep K, mean K, and KMax, and an improvement in total higher order aberrations and vertical coma (all $p < 0.001$). Reduction in KMax was greater in eyes that underwent simultaneous CXL compared to those without CXL (−4.28D vs. −0.70D; $p = 0.018$). No significant complications occurred.

Conclusions: Femto-CAIRS guided by the Brisbane nomogram provides a tailored treatment approach that improved visual acuity and regularisation of the central cornea. Further studies are required to validate our nomogram and clarify the effect of cross-linking on CAIRS.

1 | Introduction

Intracorneal ring segments (ICRS) were first introduced as a treatment for keratoconus in 2000 [1] and were subsequently widely adopted as a means of altering corneal curvature and improving visual quality in ectatic eyes. The technique of implanting these polymethyl-methacylate (PMMA) ring segments into the corneal stroma works according to Barraquer's law which states that the insertion of material into the corneal periphery will cause a flattening effect, known as an arc shortening effect, in the central cornea [2]. However, due to their synthetic nature, PMMA ICRS have been associated with a number of post-operative complications, including segment migration (0.8%–33.3%), corneal melt (0.2%–80%), and extrusion (4.7%–80%), with the overall explantation rate ranging from 1% to 19% according to a systematic review of 39 studies [3–6].

The transplantation of allogenic corneal tissue for additive keratoplasty in ectatic eyes also gained interest in the early 2000s [7–9]. The biocompatibility and malleable nature of allogenic tissue potentially offered a lower risk profile and allowed shallower implantation depth compared to synthetic ICRS. There have been various attempts at creating the ideal lenticule, including disc, crescent and donut shapes, and in 2018, Jacob

et al. first described the use of corneal allogenic intrastromal ring segments (CAIRS) for keratoconus [10]. The principle of CAIRS is to transplant a segment of donor corneal tissue into a curvilinear peripheral corneal channel to create an arc shortening effect causing central corneal flattening and regularisation.

As CAIRS transplant surgery is a relatively recent advancement, a standard nomogram for surgical planning has not yet been developed. The Istanbul nomogram has been used for manually cut full thickness CAIRS, determining the positioning of a segment of standard size and depth [11, 12], followed on by work from Bteich et al. who described a nomogram that introduced customization of effect based on varied segment width, optical zone and implantation depth according to keratoconus severity [13]. More recently, use of femtosecond laser technology for graft creation has been described which allows for further customization of both width and thickness of CAIRS segments [14–17]. This study describes a new nomogram to guide creation and implantation of femtosecond laser cut CAIRS (femto-CAIRS) and reports outcomes from its application in keratoconic eyes.

2 | Methods

This retrospective study was conducted in accordance with the tenets of the Declaration of Helsinki and was approved by the Royal Australian and New Zealand College of Ophthalmologists Human Research Ethics Committee (HREC Reference number: 173.24). Informed written consent was obtained from each patient prior to surgical intervention. The standardised consent form authorised both the procedure itself and the use of anonymized clinical data for research.

Patients aged ≥12 years with a diagnosis of keratoconus. Candidates were required to have a clear corneal stroma and a minimum central corneal thickness (CCT) of ≥300 μm. Only patients who were intolerant to rigid gas permeable contact lenses were included. Eyes were excluded if they had visually significant cataracts, pseudophakia, central or paracentral corneal scarring, prior corneal surgery (such as PTK or Keraring removal), or any other ocular disease that could affect visual outcomes. Corneal scarring and previous corneal surgery were excluded due to their potential to alter visual potential and corneal biomechanics, meaning these cases were not considered "virgin" keratoconic eyes. Eyes with advanced corneal thinning (<300 μm), previous corneal hydrops, a history of viral keratitis, or active severe allergic conjunctivitis were also excluded, as were patients with autoimmune or immunodeficiency disorders, and pregnant or breastfeeding patients. No keratometric level cut-off was required for exclusion criteria.

The surgical procedure involved a number of steps including pre-operative assessment, surgical planning, CAIRS graft preparation, and implantation. Patients had UDVA, CDVA, and subjective refraction measured preoperatively and at approximately 3, 6, 9, 12, 18 and 24 months postoperatively. CDVA was measured using spectacle correction only. Presented data are from their most recent visit. Corneal tomography was measured using the Pentacam-HD (Oculus, Germany), including flat K, steep K, mean K, topographic astigmatism, KMax, CCT, total refractive corneal power within 3 mm and 5 mm zones, and corneal aberrations including the total root mean square higher order aberrations (RMS HOA), vertical coma, and horizontal coma within 4.5 mm. Eyes were grouped solely according to keratometric values, using K-value thresholds derived from the keratometry component of Amsler–Krumeich scale [18]. They were classified as follows: Grade 1: mean $K < 48.0$ D; Grade 2: mean K 48.0–53.0 D; Grade 3: mean $K > 53.0$ D; and Grade 4: mean $K > 55.0$ D. In addition, preoperative CDVA was stratified into three study-defined categories for subgroup analysis: 0.1 logMAR or better (6/7.5); 0.2–0.4 logMAR (6/9.5–6/15); 0.5 logMAR or worse (6/19 or worse).

2.1 | Surgical Planning

CAIRS planning with the Brisbane nomogram involves three steps. The first step is to bisect the cornea with the steepest inferior area centred in the inferior half. The central axis of the segment should be perpendicular to this line. Flattening occurs centrally from the segment. Step 2 is to decide if one or two segments are needed. If one side of the cornea is flat (paracentral Ks < 44D), only one segment is required (Figure 1A). If the cornea has steepening on both sides (with Ks of ≥44D on both sides of the apex), then two segments are required (Figure 1B). The arc length of the segment is extended from the central axis, across the area where the average Ks are ≥43D in the 5 mm optic zone.

Step 3 is application of the Brisbane nomogram (Table 1) which defines the cross-sectional dimensions of the segment according to the paracentral steepest keratometry on the sagittal curvature map. The nomogram was derived from our first 32 CAIRS cases, which were not included in this analysis. It was initially based on a full-thickness allogeneic segment (550 μm × 1.0 mm), now defined as the extra-large size, and early tunnel parameters followed the technique described by Jacob et al. [10] Because existing nomograms largely targeted advanced keratoconus, progressively smaller segments were developed to treat milder disease. The nomogram was designed so that the cross-sectional area of an extra-large size segment would represent 100% and each decreasing size was a 25% reduction in this area. The channel dimensions decrease in size as the segment width and cross section decrease, so that the width of the channel is 100 μm wider than the segment. The channel depth is set at 250 μm in all cases. Where two segments are used, the width and arc length of the superior segment can be varied as needed where there is asymmetry between the superior and inferior topography. No CAIRS segment tapering was performed in this study.

2.2 | Graft Preparation

The Alcon Wavelight FS200 (Alcon Laboratories, USA) was used for both CAIRS preparation and recipient channel creation. For the graft harvest, two sequential anterior lamellar keratoplasty (ALK) profiles were planned, each comprising a circular horizontal plane formed at a specific depth and diameter in the donor cornea, followed by a circular vertical side cut beginning at the outer edge of the first cut and proceeding up to the corneal surface (Figure 2). This created a disc with a modifiable diameter and thickness. The angle between the floor and walls of

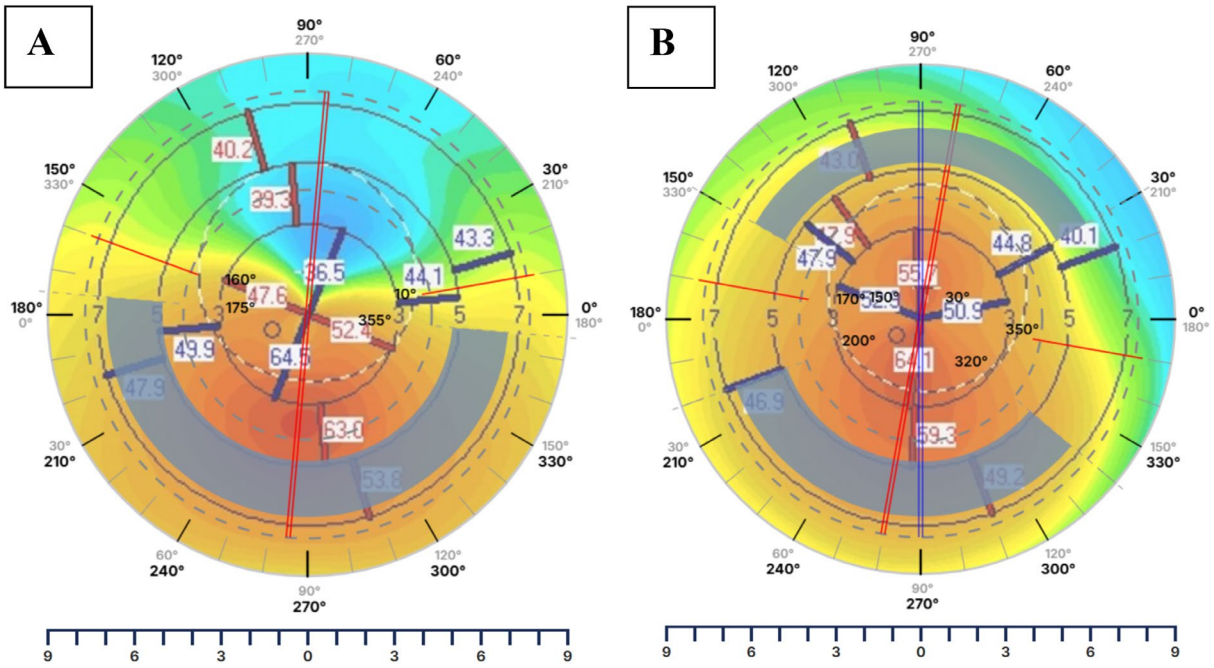

FIGURE 1 | Topographic example of an eye with inferior steepening only, requiring 1 segment (A), and an eye with superior and inferior steepening, requiring 2 segments (B).

TABLE 1 | Femto-CAIRS parameters for use with the Brisbane nomogram.

Size	Small	Medium	Large	Extra large
Segment width (μm)	700	800	900	1000
Segment thickness (μm)	200	300	400	500
Cross sectional area (mm^2)	0.14	0.24	0.36	0.50
Channel inner diameter (mm)	4.8	4.6	4.5	4.4
Channel outer diameter (mm)	7.0	7.0	7.3	7.6
Resulting channel width (mm)	1.1	1.2	1.4	1.6
Inferior cone apex keratometry (D)	46–48	48–50	50–55	> 55

the incisions was set to 90 degrees. The first profile (outer ALK) sets the outer wall diameter of the ring and the depth of the cut defines the vertical thickness. The second profile (inner ALK) was created with a smaller diameter to form the inner wall of the ring segment. The width of the ring segment was defined by the relationship: ring width = (outer ALK diameter—inner ALK diameter)/2. The depth of the inner cut was set at 50 μm deeper than the outer cut to ensure a complete incision.

The WaveLight FS 200 was in a temperature and humidity-controlled day hospital procedure room. A sterile field was placed over the FS200 calibration head unit and sterile handle covers were placed over the bed control and FS200 joysticks. A viable corneal graft was placed onto a Barron artificial anterior chamber (Katena Products, USA). Each full thickness graft was determined to be viable according to the Eye Bank Association of Australian and New Zealand standards according to serology, endothelial cell density, tissue clarity, and structural integrity. A single corneal graft was used for each patient to generate 1 or 2 rings. The endothelium was removed from all grafts to eliminate immunogenic endothelial cells and minimise the risk of allograft-related immune reactions.

Cellulose eye spears were used to remove the epithelium from the graft. The centre of the graft was marked with a very fine ink mark. A clamp was used to occlude the vacuum tubing on the FS200 interface ring to allow docking and obtaining Vacuum 1. The laser was docked onto the artificial anterior chamber and Vacuum 2 was obtained. Once docked, the digital reticule was centred onto the preplaced mark. The outer ALK profile was completed, and the artificial anterior chamber was repressurized with BSS. The interface was changed and the procedure was repeated for the inner ALK profile. Care was taken to ensure on repeat docking that horizontal movements were minimised to avoid warping the graft. The produced ring was then measured with a Mendez marker (Katena Products, USA) and the desired clock hour segment divided with Vannas scissors (Katena Products, USA). The Bowmans surface was marked with 5–8 fine ink spots and then it was placed Bowmans side down on a sterile plastic surface to dehydrate for 5 min.

2.3 | CAIRS Implantation

The centre of the pupil and orientation axis were marked with the patient at the slit lamp. The patient was then positioned

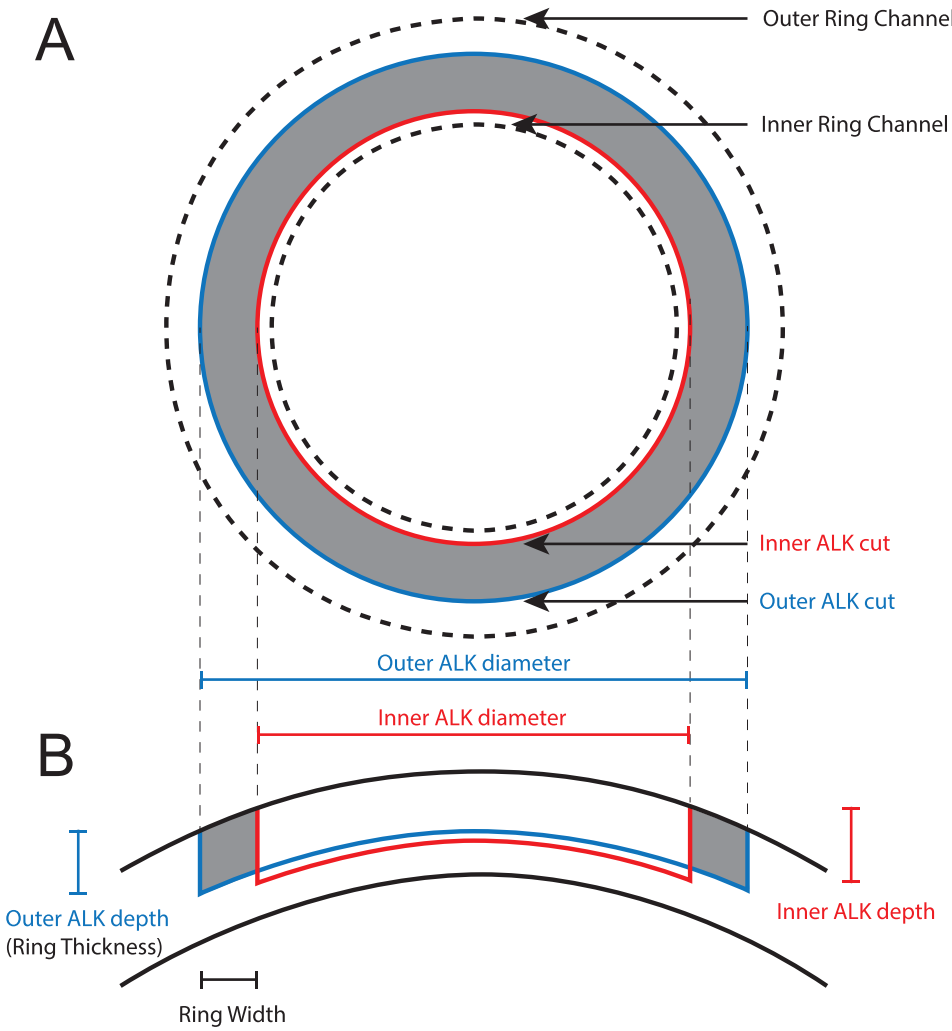

FIGURE 2 | Diagram of the femto-CAIRS creation from above (A) and in cross section (B). Three profiles are shown: The first is the outer ALK cut (blue), the second is the inner ALK cut (red), and the third is the ring channel profile that is performed on the recipient to prepare for implantation (dashed lines in (A)). The inner and outer ALK cut create the segment (grey). ALK, anterior lamellar keratotomy.

under the laser microscope, draped, and a corneal ring profile was performed to create a channel at a depth of 250 μm and optical zone dimensions that were defined by the nomogram in Table 1. Two vertical incisions were desired to place the segment with ease. As the FS200 only allows one incision to be programmed, a second opposing incision was formed manually using a 350 μm accurate depth knife (Geuder AG, Germany). The channel was opened using an iris spatula and the CAIRS segment was inserted into the channel ensuring that it was stretched to its natural length and not twisted by using the ink spots as visual guides. Operating microscope keratoscopy was used to check central corneal regularity and the segment orientation was adjusted if required. Subconjunctival cefazolin and dexamethasone were used. Postoperatively, patients were prescribed the following eye drops: tobramycin 0.3% four times daily for 7 days, dexamethasone 0.1% four times daily for 28 days, and lubricants as required.

The femtosecond laser–assisted procedure required three separate patient interface dockings to complete all femtosecond cutting steps.

2.4 | Corneal Cross-Linking

Eyes were grouped based on their cross-linking (CXL) status; 18 eyes had CXL prior to CAIRS (P-CXL), and 27 eyes did not require CXL (no evidence of progression) (N-CXL). For 40 eyes, there was prior evidence of progression and no history of CXL, of these, 30 eyes had simultaneous CXL (S-CXL), and 10 had CXL at least 3 months after CAIRS. For these 10 eyes, the timing of CXL was delayed due to patient scheduling and logistical factors, and was not based on postoperative assessment of keratoconus progression. For eyes that had CXL more than 3 months after CAIRS, their pre-CXL data was used in the analysis. For eyes that underwent S-CXL, all treatments were an oxygen-enriched transepithelial-accelerated CXL protocol which has been previously described [10]. Briefly, the 2-step topical application of ParaCel riboflavin (Avedro Inc., USA) was followed where 0.25% riboflavin (ParaCel Part 1) was instilled every 60 s for 4 min, followed by 0.22% riboflavin (ParaCel Part 2) every 30 s for 6 min. Oxygen delivery goggles (Boost, Avedro Inc., USA) then delivered supplemental oxygen to the eye at a flow rate of 1.5–2.5 L/min with concurrent

pulsed ultraviolet A (1 s on, 1 s off, 30 mW/cm^2, 365 nm) using the Avedro KXL II system (Glaukos, USA) to deliver a total energy dose of 10 J/cm^2.

2.5 | Statistical Analyses

Statistical analyses were performed using SPSS version 30.0 (IBM SPSS Inc.). Continuous variables are presented as mean ± standard deviation, and categorical variables as frequencies and percentages. Normality of continuous variables was assessed using the Shapiro–Wilk test. Preoperative and postoperative measurements were compared using the Wilcoxon signed-rank test. Between-group comparisons were conducted using a mixed-effects model, with postoperative month as covariate to account for varying follow-up timepoints and patient treated as a cluster variable to account for inter-eye correlation [19, 20]. All post hoc pairwise comparisons were adjusted using the Bonferroni correction. A p-value < 0.05 was considered statistically significant.

TABLE 2 | Patient demographics and preoperative measurements. Data presented as mean ± SD or *n* (%).

Patients	
N	75
Age (years)	40.0 ± 15.8
Sex	
Male	50 (66.7%)
Female	25 (33.3%)
Eyes	
N	85
Laterality	
Left	41 (48.2%)
Right	44 (51.8%)
Preoperative parameters	
Visual acuity	
0.1 logMAR or better	0.06 ± 0.06 (*n* = 27, 31.8%)
0.2–0.4 logMAR	0.28 ± 0.07 (*n* = 37, 43.5%)
0.5 logMAR or worse	0.67 ± 0.21 (*n* = 21, 24.7%)
Keratometric grading	
1	38 (44.7%)
2	27 (31.8%)
3	7 (8.2%)
4	13 (15.3%)
Cross-linking status	
No CXL	37 (43.5%)
Prior CXL	18 (21.2%)
Simultaneous CXL	30 (35.3%)

3 | Results

The Shapiro–Wilk test showed that most variables were not normally distributed, with only age, UDVA, and CCT (preop), refractive astigmatism and vertical/horizontal coma (paired differences), and refractive astigmatism and KMax (between groups) meeting normality. Paired comparisons were analysed using the Wilcoxon signed-rank test, while between-group comparisons of baseline data and change in continuous variables were performed using a mixed-effects model, which is robust to non-normal data, with groups defined by CXL status, preoperative CDVA, and KCN severity.

Table 2 describes the patients' demographics. Data from 85 eyes from 75 patients were analysed. Ten patients (13.3%) underwent bilateral surgery. The mean age of patients at the time of surgery was 40.0 ± 15.8 years (*range* 12.0–66.3 years), and 50 (66.7%) were male. Data are presented from the most recent postoperative visit which was 7.5 ± 5.0 months after surgery (*range* 3–32 months). Details of the segment size, length, and implantation depth are presented in Table 3.

TABLE 3 | CAIRS transplantation data for all eyes (*n* = 85).

Parameter	Category	*n* (%)
Number of segments implanted	1 Segment	68 (80%)
	2 Segments	17 (20%)
Segment size	Small (S)	0 (0%)
	Medium (M)	30 (35.3%)
	Large (L)	36 (42.4%)
	Extra large (XL)	19 (22.4%)
Angular length (degrees)	90°	3 (3.5%)
	105°	3 (3.5%)
	120°	22 (25.9%)
	135°	7 (8.2%)
	140°	1 (1.2%)
	150°	18 (21.2%)
	160°	5 (2.9%)
	165°	8 (9.4%)
	180°	6 (7.1%)
	195°	1 (1.2%)
	210°	3 (3.5%)
Implantation depth (% of CCT)	45%–49%	3 (3.5%)
	50%–54%	34 (40.0%)
	55%–59%	26 (30.6%)
	60%–64%	15 (17.6%)
	65%–69%	3 (3.5%)
	70%–80%	4 (4.7%)

TABLE 4 | Comparison of preoperative demographic and topographic data for each CXL group. *p* Values were calculated using a mixed-effects model, adjusted with the Bonferroni correction.

	No-CXL	P-CXL	S-CXL	*p*
Age (years)	42.5 ± 11.2	29.0 ± 9.3	31.0 ± 11.9	< 0.001
SE (D)	−3.60 ± 3.68	−3.09 ± 4.26	−3.79 ± 4.61	0.860
UDVA (logMAR)	0.9 ± 0.3	0.9 ± 0.4	0.8 ± 0.4	0.274
CDVA (logMAR)	0.3 ± 0.2	0.4 ± 0.3	0.3 ± 0.2	0.552
Steep K (D)	51.1 ± 4.5	54.6 ± 7.3	51.0 ± 5.0	0.050
Flat K (D)	46.6 ± 3.9	49.6 ± 5.0	47.0 ± 3.8	0.041
KMax (D)	57.0 ± 5.8	62.0 ± 8.2	57.9 ± 7.4	0.019
CCT (μm)	451 ± 34	430 ± 50	445 ± 46	0.072

Abbreviations: CCT, central corneal thickness; CDVA, corrected distance visual acuity; CXL, corneal collagen cross-linking; D, diopters; K, keratometry; KMax, maximum keratometry; logMAR, logarithm of the minimum angle of resolution; P-CXL, prior CXL; S-CXL, simultaneous CXL; SE, spherical equivalent; UDVA, uncorrected distance visual acuity; μm, micrometres.

Table 4 shows comparisons between preoperative age, SE, VA, keratometry, and CCT for each CXL group. Post hoc analyses revealed a difference in age between the No-CXL and P-CXL groups, and No-CXL and S-CXL groups (both $p < 0.001$). Preoperative flat K and KMax were slightly lower in the No-CXL compared to the P-CXL group ($p = 0.046$ and $p = 0.017$).

Figure 3 shows the change in Snellen lines of acuity for both UDVA and CDVA. UDVA improved by an average of 4 lines, with the greatest improvement being 13 lines. There was an improvement of 5 or more lines in 31 eyes (43.7%), 8 eyes (11.3%) had no change in UDVA, 1 eye lost 1 line and 1 eye lost 2 lines of UDVA.

CDVA improved by an average of 2 lines, with the greatest improvement being 11 lines. There was no change in CDVA for 12 eyes (14.1%), 4 eyes (4.7%) lost 1 line of CDVA, and one eye (1.2%) lost 2 lines. Of the 12 eyes that had no change in CDVA, 10 had a preoperative CDVA of between −0.1 and 0.1 logMAR. Of the 5 eyes that lost lines of CDVA, there was a reduction of refractive astigmatism of between 0.25D and 3.25D.

Table 5 shows the preoperative and postoperative values for each measured outcome. There was an improvement in visual acuity and refractive error, as well as significant corneal flattening and a reduction in corneal power. There was a significant improvement in both the manifest refraction spherical equivalent (SE) (2.66 D, $p < 0.001$) and the refractive astigmatism (1.44 D, $p < 0.001$). The greatest improvement in SE was 14.25 D, and there was a reduction of 3 D or more in 27 eyes (31.8%). The greatest improvement in refractive astigmatism was 9.50 D and there was a reduction of 2 D or more in 34 eyes (40.0%).

KMax reduced by 5D or more in 21 eyes (24.7%) and the maximum reduction was 18.6D. Steep K reduced by 5D or more in 31 eyes (36.5%). There was only a small improvement in topographic astigmatism (0.6D, $p = 0.003$), however 29 eyes (34.1%) had an improvement of 1D or more. The mean power of the cornea decreased across both the central 3 mm (5.4D, $p < 0.001$) and 5 mm (4.3D, $p < 0.001$). There was a small increase in CCT (4 μm, $p = 0.013$).

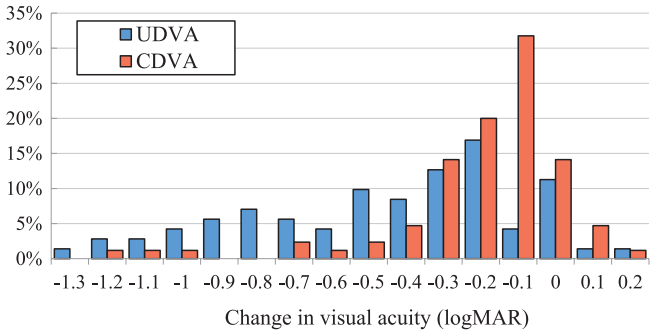

FIGURE 3 | Change in visual acuity after CAIRS for both uncorrected distance visual acuity (UDVA) and corrected distance visual acuity (CDVA). Negative change on a logMAR scale indicates improvement in visual acuity.

Total RMS HOA and vertical and horizontal coma were measured within central 4.5 mm. There was a significant reduction in the total RMS HOA (0.37, $p < 0.001$) as well as in vertical coma (0.564, $p < 0.001$). There was an increase in horizontal coma which changed from a negative to a positive value (temporal to nasal distortion change) (0.179, $p = 0.038$).

Table 6 shows the change in each parameter, grouped by CXL status and adjusted for the difference in age, flat K, and KMax between groups. There was no significant difference in the change in visual acuity, steep K, flat K, mean K, topographic astigmatism, or pachymetry between groups. The only difference across groups was the reduction in refraction, which was greater in the No-CXL group compared to the P-CXL group (0.78D vs. 2.32D, $p = 0.035$) and KMax, which was greater in the S-CXL group compared to the No-CXL group (−4.28D vs. −0.70D, $p = 0.026$). No intraoperative or postoperative complications occurred, and there were no cases of corneal melt over the segment or segment extrusion. Examples of the preoperative and postoperative topography, as well as the surgical planning diagram, are provided for 3 eyes (Figures 4–6).

The change in each parameter was also analysed according to the preoperative CDVA (0.1) logMAR or better (6/7.5); 0.2–0.4 logMAR (6/9.5–6/15); 0.5 logMAR or worse (6/19 or worse): and

TABLE 5 | Preoperative and postoperative measures of visual acuity, refraction, corneal tomography, pachymetry, and corneal aberrations ($n = 85$). p Values were calculated using the Wilcoxon signed-rank test.

Parameter	Pre/post operative	Minimum	Maximum	p
UDVA (logMAR)				
Preoperative	0.8 ± 0.3	0.2	1.5	< 0.001
Postoperative	0.4 ± 0.3	−0.1	1.1	
CDVA (logMAR)				
Preoperative	0.3 ± 0.3	−0.1	1.3	< 0.001
Postoperative	0.1 ± 0.2	−0.1	0.8	
Spherical equivalent (D)				
Preoperative	−3.56 ± 4.11	−17.38	5.38	< 0.001
Postoperative	−0.90 ± 2.37	−9.50	2.50	
Refractive astigmatism (D)				
Preoperative	−4.57 ± 2.15	−11.50	0.00	< 0.001
Postoperative	−3.13 ± 1.90	−8.25	0.00	
Steep K (D)				
Preoperative	51.8 ± 5.5	43.7	73.6	< 0.001
Postoperative	47.4 ± 3.9	42.1	59.1	
Flat K (D)				
Preoperative	47.4 ± 4.2	39.4	58.2	< 0.001
Postoperative	43.6 ± 3.4	37.2	58.5	
Mean K (D)				
Preoperative	49.5 ± 4.6	41.9	64.8	< 0.001
Postoperative	45.4 ± 3.5	39.5	58.8	
KMax (D)				
Preoperative	58.4 ± 7.1	45.4	83.0	< 0.001
Postoperative	55.9 ± 6.2	45.4	77.6	
Topographic astigmatism (D)				
Preoperative	−4.4 ± 2.7	−15.9	−0.2	0.003
Postoperative	−3.8 ± 2.4	−10.9	−0.3	
CCT (μm)				
Preoperative	446 ± 42	305	549	0.013
Postoperative	450 ± 46	309	531	
Corneal power 3 mm (D)				
Preoperative	49.1 ± 4.3	41.2	58.8	< 0.001
Postoperative	43.7 ± 3.5	38.2	58.2	
Corneal power 5 mm (D)				
Preoperative	48.6 ± 3.8	41.2	60.2	< 0.001
Postoperative	44.3 ± 3.1	40.0	57.6	

(Continues)

TABLE 5 | (Continued)

Parameter	Pre/post operative	Minimum	Maximum	*p*
Total RMS HOA (μm)				
Preoperative	1.500 ± 0.595	0.435	3.347	< 0.001
Postoperative	1.130 ± 0.623	0.215	3.520	
Vertical coma (μm)				
Preoperative	−1.264 ± 0.688	−3.302	0.725	< 0.001
Postoperative	−0.700 ± 0.768	−2.928	0.869	
Horizontal coma (μm)				
Preoperative	−0.010 ± 0.603	−1.352	1.676	0.038
Postoperative	0.169 ± 0.493	−0.924	1.745	

Abbreviations: CCT, central corneal thickness; CDVA, corrected distance visual acuity; D, diopters; HOA, higher-order aberrations; KMax, maximum keratometry; logMAR, logarithm of the minimum angle of resolution; RMS, root mean square; UDVA, uncorrected distance visual acuity; μm, micrometres.

TABLE 6 | Comparison between the change in visual acuity, refraction, corneal topography, and pachymetry by CXL status. *p* Values were calculated using a mixed-effects model, adjusted with the Bonferroni correction.

Parameter	No-CXL (*n* = 37)	Prior-CXL (*n* = 18)	S-CXL (*n* = 30)	*p*-Value a vs. b	*p*-Value a vs. c	*p*-Value b vs. c
UDVA (logMAR)	−0.4 ± 0.4	−0.6 ± 0.3	−0.4 ± 0.3	0.243	1.000	0.650
CDVA (logMAR)	−0.2 ± 0.2	−0.2 ± 0.3	−0.2 ± 0.2	1.000	1.000	1.000
SE (D)	2.68 ± 2.90	2.43 ± 3.50	2.78 ± 3.87	1.000	1.000	1.000
Refractive astigmatism (D)	0.78 ± 2.22	2.32 ± 1.92	1.73 ± 2.45	0.035	0.200	1.000
Steep K (D)	−3.86 ± 2.79	−5.67 ± 3.56	−4.30 ± 2.70	0.116	1.000	0.351
Flat K (D)	−3.66 ± 2.09	−4.31 ± 2.59	−3.64 ± 2.69	0.909	1.000	1.000
Mean K (D)	−3.76 ± 2.17	−4.91 ± 2.37	−3.96 ± 2.65	0.268	1.000	0.583
KMax (D)	−0.70 ± 4.40	−3.07 ± 5.91	−4.28 ± 4.42	0.314	0.026	1.000
Topographic astigmatism (D)	0.2 ± 2.2	1.4 ± 4.0	0.7 ± 1.1	0.397	1.000	0.944
CCT (μm)	3 ± 16	8 ± 21	2 ± 20	0.673	1.000	1.000

Abbreviations: CCT, central corneal thickness; CDVA, corrected distance visual acuity; CXL, cross-linking; D, diopters; KMax, maximum keratometry; S-CXL, simultaneous cross-linking; SE, spherical equivalent; UDVA, uncorrected distance visual acuity.

keratometry grading. These results are shown in Table 7. There was a greater improvement in CDVA, spherical equivalent, steep K, flat K, and mean K for eyes that had a worse preoperative CDVA (0.5 logMAR or worse; 6/19 or worse).

Similarly, comparisons across keratometric severity grades showed that eyes with more advanced preoperative steepening exhibited greater postoperative effect. Significant differences were observed for spherical equivalent, refractive astigmatism, steep K, flat K, mean K, and central corneal thickness ($p = 0.002$). UDVA, CDVA, KMax, and topographic astigmatism, however, did not vary significantly between keratometric severity groups.

4 | Discussion

This study presents a novel approach to surgical planning for femto-CAIRS using the Brisbane nomogram to determine the segment width, thickness, axis, and arc length based on the individual corneal topography. Since it was first described in 2023 [17], there have been only two published studies examining the outcomes of femto-CAIRS [14, 16]. The main benefit of using femtosecond laser to create each segment is that it allows precise and repeatable customization of the width, thickness, and radius of curvature of each segment and removes the potential variable of donor corneal thickness inherent in trephine-derived segments. The main drawback is the availability and affordability of femtosecond laser technology. Although it is possible to perform CAIRS surgery without a femtosecond laser [21], this method likely offers less precision in channel width, depth, and centration compared to femto-CAIRS. It may also require more time and surgical skill to perform and may carry a higher risk profile for some intraoperative and postoperative complications.

While Bteich et al. used the same nomogram as for manually cut CAIRS with only two options for segment thickness (500 and

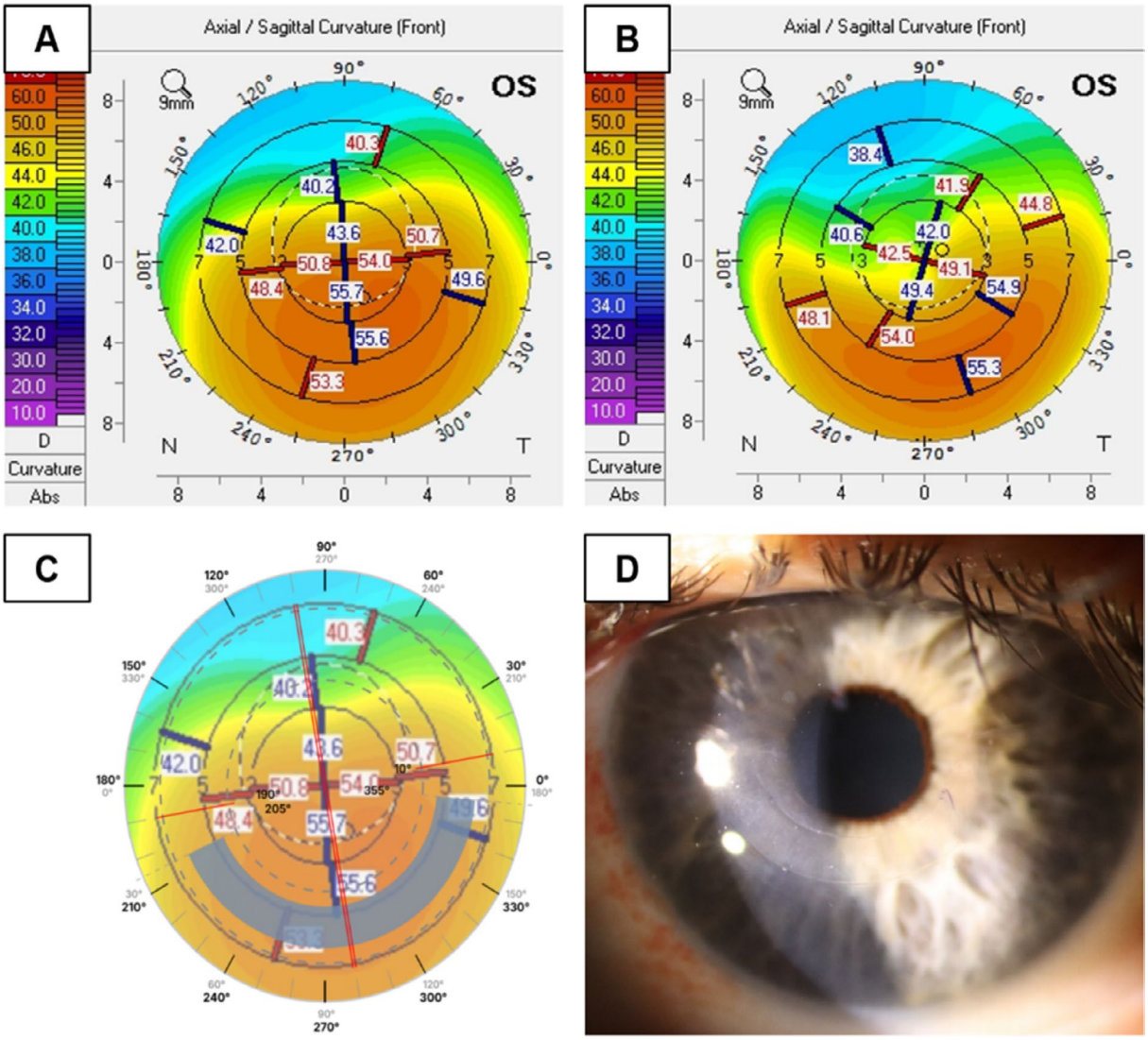

FIGURE 4 | Preoperative axial curvature (A), postoperative axial curvature (B), CAIRS placement (C), and postoperative slit lamp image (D) for an eye with preoperative keratoconus severity grade 2. This eye had postoperative improvements in UDVA and CDVA of 1.1 logMAR and 0.1 logMAR, respectively. CAIRS, corneal allogenic intrastromal ring segments; UDVA, uncorrected distance visual acuity; CDVA, corrected distance visual acuity; logMAR, logarithm of the minimum angle of resolution.

750 μm) [16], the nomogram used by Mechleb et al. involved four options for thickness between 500 and 1200 μm selected based on keratometry, and while they did not provide the exact details, the arc length of the segment was determined according to the subjective refraction and axis according to the steep meridian, axis of coma, and axis of the topographic astigmatism [14]. Use of subjective refraction in a nomogram may be problematic due to the high degree of variability in subjective refraction in keratoconic eyes [22].

Improvements in visual acuity align closely with previous reports of both trephine-derived and femto-CAIRS where UDVA improved by an average of between 3 and 5 lines, and CDVA by 1 to 4 lines [10, 13, 14, 16, 23], and are comparable to those achieved with synthetic ICRS [24]. CDVA improved by 1 or more lines in 80.0%, and by 3 or more lines in 28.2% of eyes. This proportion of eyes that gained 3 or more lines is lower than in previous reports of femto-CAIRS [14, 16], likely due to the large proportion of eyes with a preoperative CDVA of 0.1 or better (37.5%) in the current study, limiting the potential for larger improvements. Of the 5 eyes (5.9%) which lost 1 or 2 lines of CDVA, 4 had significant reductions in their refractive error, reduced anisometropia, and improved spectacle tolerance. Comparatively, Mechleb [14] reported that 13.7% of eyes lost lines of CDVA at 3 months post femto-CAIRS.

The topographic and refractive changes post CAIRS vary considerably according to the severity of keratoconus, preoperative refractive error, thickness, depth, arc length and positioning of the segment. While the average reduction in SE and KMax was 2.66D and 2.50D, the maximum changes were as large as 14.25D and 18.6D, respectively. The average reduction in KMax and mean K agrees with previously published CAIRS studies where there was a reported reduction in KMax of 1.7D to 5.6D and Mean K of 3.4D to 4.2D [10, 13, 14, 16, 23]. KMax was highly variable in the study cohort, likely due to the localised peripheral steepening seen from the CAIRS segment. For centrally placed segments combined with a large scan, it

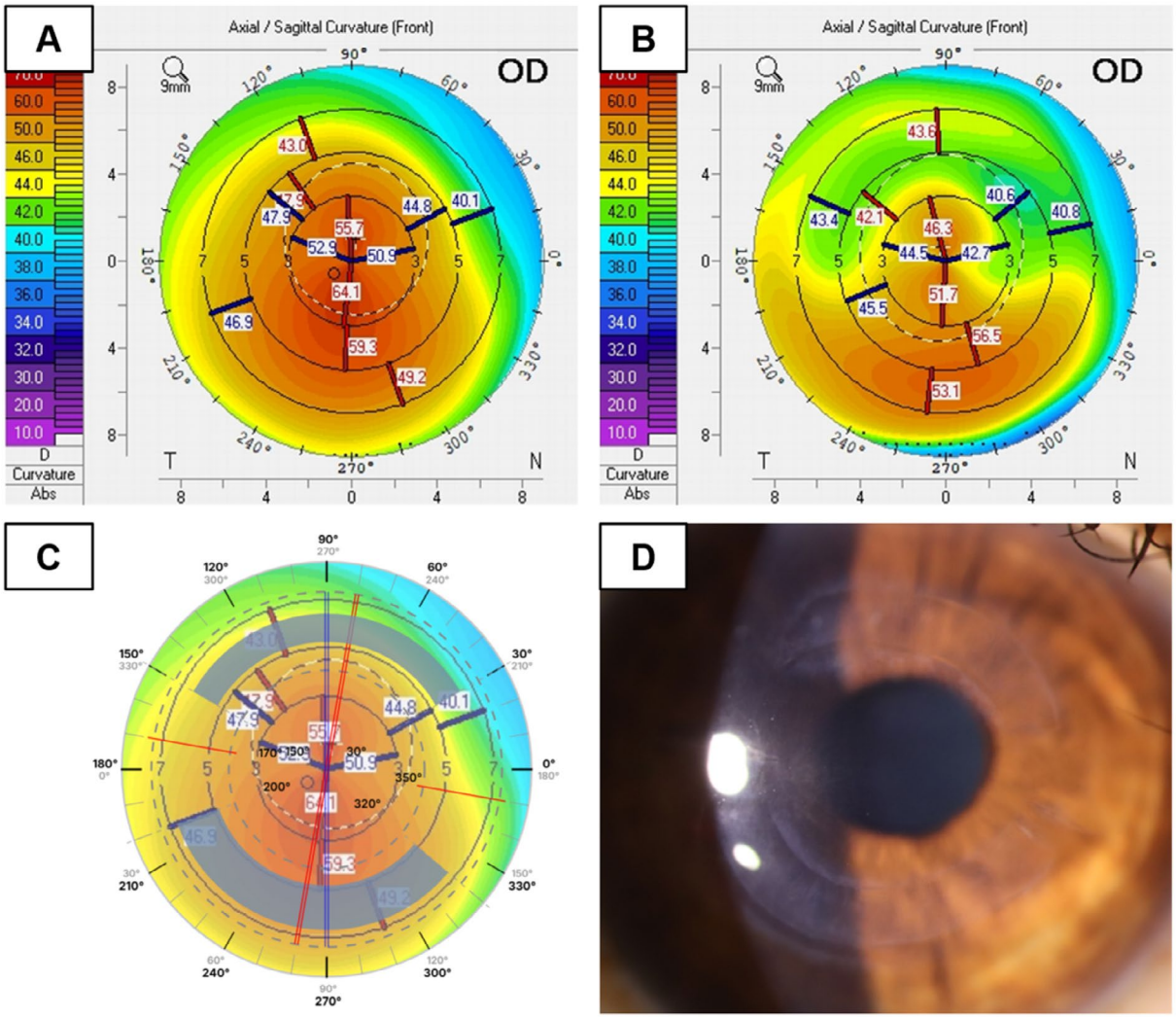

FIGURE 5 | Preoperative axial curvature (A), postoperative axial curvature (B), CAIRS placement (C), and postoperative slit lamp image (D) for an eye with preoperative keratoconus severity grade 3. This eye had postoperative improvements in UDVA and CDVA of 0.3 logMAR and 0.3 logMAR, respectively. CAIRS, corneal allogenic intrastromal ring segments; UDVA, uncorrected distance visual acuity; CDVA, corrected distance visual acuity; logMAR, logarithm of the minimum angle of resolution.

was not uncommon to detect this topographic effect and an associated increase in KMax despite central flattening and reduction in central Ks.

In our study, eyes with poorer baseline CDVA (≥0.5 logMAR) exhibited greater postoperative improvements in refractive error and keratometric flattening compared with eyes that had good preoperative vision. Likewise, the greater magnitude of postoperative flattening was observed in higher keratometric severity groups (Grades 3–4). A similar effect occurs in synthetic ICRS due to the arc-shortening effect. In this article, the depth of implantation was kept constant at 250 μm, which corresponded to a depth of 50%–63% of the total CCT for the majority of eyes (85%). Given that shallower segments are possible with CAIRS and are likely to result in a greater degree of flattening, this should be investigated in future research.

For 17 eyes with steepening in both the inferior and superior cornea, two segments were used, positioned across the steepest areas. This differs from synthetic ICRS which are often placed nasally and temporally in such cases. Early clinical experience of the authors found undercorrection of astigmatism in cases where incisions were placed on the steep axis and segments positioned on the flat axis. CAIRS implants seem to flatten the cornea centrally from their placement and so had a better regularisation effect when positioned on the steep axis of the astigmatism. This difference may be due to the lack of rigidity of the CAIRS implants and less induction of a "splinting" effect that acrylic ICRS may cause.

A significant degree of reduced visual quality in keratoconus can be attributed to HOAs [25] and it follows that the reduction in aberrations achieved with CAIRS surgery leads to a significant improvement in visual quality. This study found an improvement in the total HOA as well as the vertical coma measured within a central 4.5 mm zone. The mean horizontal coma changed from −0.010 to 0.169 μm, indicating a shift in image distortion from the temporal to nasal side. Previous reports of both trephine-derived CAIRS [13, 23], and femto-CAIRS [14, 16] described an improvement in total HOA and vertical coma, but no change in horizontal coma. Future research should analyse the relationship between segment width and positioning and HOAs across different zones of the cornea.

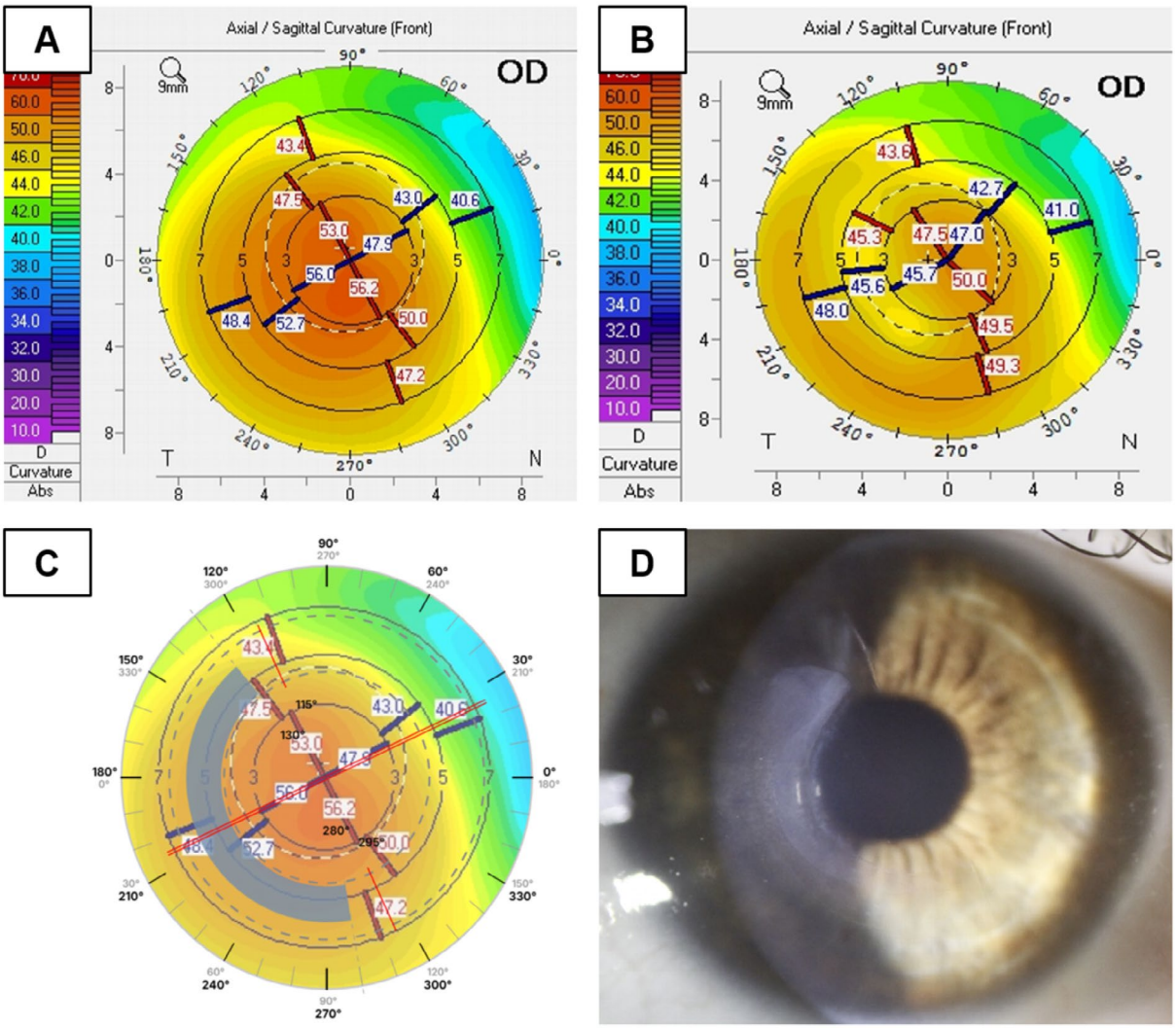

FIGURE 6 | Preoperative axial curvature (A), postoperative axial curvature (B), CAIRS placement (C), and postoperative slit lamp image (D) for an eye with preoperative keratoconus severity grade 2. This eye had postoperative improvements in UDVA and CDVA of 0.8 logMAR and 0.5 logMAR, respectively. CAIRS, corneal allogenic intrastromal ring segments; UDVA, uncorrected distance visual acuity; CDVA, corrected distance visual acuity; logMAR, logarithm of the minimum angle of resolution.

It has been suggested that due to the stiffening effect of CXL, CAIRS surgery may have a lesser effect on eyes with prior CXL [26], The results of this study do not confirm this theory, as there was no significant difference in surgical outcomes between eyes with prior CXL compared to those without. There was found to be a greater reduction in KMax in eyes that underwent simultaneous CXL compared to the eyes that did not undergo CXL, suggesting that combining the two procedures has a greater corneal flattening effect. These comparisons are limited by the small number of eyes in each group; therefore, larger studies are needed to further explore the relationship between CXL and CAIRS outcomes. To date, there has been no consensus on the most appropriate timing for CXL when indicated and, as such, decisions are made on a case-by-case basis. Although not described to our knowledge, a potential concern with performing CXL after CAIRS surgery is that post-CXL corneal thinning may lead to compromise of the tunnel roof, which could theoretically lead to graft extrusion. Although no cases of extrusion or melt occurred in this study, future research should investigate the degree of corneal thinning that occurs of the graft or tunnel roof in post-CAIRS CXL.

One alternative surgical option to CAIRS is topography-guided phototherapeutic keratectomy (PTK). The typical protocol involves a topographic PTK using a partial refractive correction, limiting the maximum ablation to 50 μm and aiming to flatten and regularise the central 5 mm [27]. Long-term studies have reported an average reduction in the steep K of 4.70D, KMax of 7.26D, an improvement in UDVA of 4 lines, and CDVA of 1 line, and improvements in HOAs [27–30]. While these visual and topographic outcomes may be similar to CAIRS, a significant drawback to PTK in ectatic eyes is the ablation of tissue in an already thin cornea. This treatment is irreversible and there are limitations in patient eligibility related to corneal thickness. In contrast, CAIRS is tissue sparing, reversible and can be performed in eyes with advanced keratoconus and corneal thickness under 400 μm.

When our centre commenced CAIRS surgery in 2021, non-viable or pre-prepared corneal tissue specifically designed for CAIRS was not yet available in Australia, and there were no established protocols for tissue selection in fully femtosecond

TABLE 7 | Comparison between the change in visual acuity, refraction, corneal topography, and pachymetry by preoperative CDVA and keratoconus severity. *p* Values between groups were calculated using a mixed-effects model.

	Preop CDVA			
Parameter	**0.1 logMAR or better (6/7.5) (*n* = 27)**	**0.2–0.4 logMAR (6/9.5–6/15) (*n* = 37)**	**0.5 logMAR or worse (6/19 or worse) (*n* = 21)**	***p***
UDVA (logMAR)	−0.5 ± 0.3	−0.3 ± 0.3	−0.6 ± 0.4	0.119
CDVA (logMAR)	−0.0 ± 0.1	−0.2 ± 0.1	−0.4 ± 0.3	< 0.001
SE (D)	1.26 ± 2.11	2.54 ± 2.86	4.68 ± 4.46	0.002
Refractive astigmatism (D)	1.66 ± 1.98	1.07 ± 2.65	1.81 ± 2.05	0.439
Steep K (D)	−3.40 ± 1.97	−4.36 ± 2.94	−5.76 ± 3.68	0.022
Flat K (D)	−2.75 ± 1.50	−3.87 ± 2.46	−5.00 ± 2.75	0.006
Mean K (D)	−3.05 ± 1.65	−4.09 ± 2.56	−5.35 ± 2.41	0.004
KMax (D)	−2.59 ± 3.70	−2.60 ± 5.07	−2.07 ± 6.29	0.898
Topographic astigmatism (D)	0.65 ± 1.02	0.49 ± 1.73	0.78 ± 4.23	0.839
CCT (μm)	6 ± 20	5 ± 15	−1 ± 22	0.461
	Preop K			
Parameter	**Grade 1 (*n* = 38)**	**Grade 2 (*n* = 27)**	**Grade 3 (*n* = 7)**	**Grade 4 (*n* = 13)**	***p***
UDVA (logMAR)	−0.3 ± 0.3	−0.5 ± 0.4	−0.5 ± 0.4	−0.6 ± 0.3	0.129
CDVA (logMAR)	−0.2 ± 0.2	−0.2 ± 0.2	−0.2 ± 0.2	−0.2 ± 0.3	0.968
SE (D)	1.80 ± 1.84	2.48 ± 2.50	6.04 ± 5.64	3.73 ± 5.35	0.015
Refractive astigmatism (D)	0.85 ± 1.55	1.32 ± 2.65	2.64 ± 2.05	2.77 ± 2.94	0.003
Steep K (D)	−2.91 ± 1.86	−4.80 ± 2.69	−5.50 ± 2.67	−7.33 ± 3.87	< 0.001
Flat K (D)	−2.53 ± 1.23	−3.94 ± 1.69	−5.07 ± 2.43	−6.50 ± 3.58	< 0.001
Mean K (D)	−2.70 ± 1.39	−4.34 ± 1.91	−5.26 ± 2.46	−6.88 ± 2.85	< 0.001
KMax (D)	−1.44 ± 3.35	−2.47 ± 5.43	−3.94 ± 4.13	−4.65 ± 7.50	0.091
Topographic astigmatism (D)	0.39 ± 1.30	0.88 ± 2.28	0.41 ± 1.11	0.82 ± 4.87	0.905
CCT (μm)	1 ± 17	13 ± 14	−2 ± 18	−6 ± 24	0.002

Note: Preop K severity; Grade 1: mean K < 48.0 D; Grade 2: mean K 48.0–53.0 D; Grade 3: mean K > 53.0 D; and Grade 4: mean K > 55.0 D.
Abbreviations: CCT, central corneal thickness; CDVA, corrected distance visual acuity; D, diopters; KMax, maximum keratometry; K, keratometry; logMAR, logarithm of the minimum angle of resolution; SE, spherical equivalent; UDVA, uncorrected distance visual acuity.

laser–assisted CAIRS. For this reason, we deliberately used viable eye-bank donor tissue to ensure consistent tissue quality and near-physiologic thickness to minimise potential variability in femtosecond cut precision and implant geometry during development of the Brisbane nomogram.

As our experience increased, and in consultation with our local tissue bank, from 2023 onwards, we transitioned to non-viable tissue as routine practice. Around this time commercially prepared non-viable CAIRS tissue also became available. This transition occurred outside the cohort analysed in the present study and was therefore not evaluated or reported. To maintain methodological consistency and avoid introducing unanalysed heterogeneity, only eyes treated with viable donor tissue were included in this manuscript. We agree that tissue source is an important consideration for future CAIRS studies, and our subsequent clinical experience suggests that high-quality non-viable tissue supplied at near-physiologic thickness can yield comparable outcomes, although this warrants formal investigation.

This study has several limitations. First, the sample size was relatively small, and research is ongoing that will contribute to larger cohorts of femto-CAIRS outcomes in the future. Second, follow-up duration was limited. As the flattening effect of CXL is known to continue for at least 12 months [31], and postoperative stromal remodelling around the implanted segments may also occur during the later postoperative period, additional topographic changes may emerge with longer observation. The longest published follow-up for CAIRS to date is 3 years, and therefore long-term stability and safety remain unknown [32].

A key limitation of this study is that postoperative outcomes were analysed using the most recent available visit for each eye rather than standardised postoperative time points (e.g., 3, 6, or

12 months). To address these limitations in the current dataset, we employed a mixed-effects model, which is particularly well suited for handling unbalanced data, such as when different eyes have only a single postoperative time point. In the model, postoperative month was included as a covariate so that any variability associated with timing was accounted for when comparing groups. At this stage, assessment of predictability is limited by the variability in preoperative keratoconus severity and the multiple surgical variables involved. A substantially larger study population would be required to draw statistically meaningful conclusions regarding predictability. Future research should examine the influence of preoperative corneal biomechanics on femto-CAIRS outcomes, including comparisons between eyes with and without prior CXL. In addition, incorporating a validated patient-reported outcome questionnaire to evaluate subjective changes in quality of vision is warranted.

CAIRS keratoplasty and the nomograms used to guide segment selection remain areas of rapidly evolving knowledge. The nomogram we used in the current study is not intended to be universally applicable or definitive; rather, it illustrates that a single standardised approach is unlikely to suit all keratoconic corneas, and that even mild keratoconus can be effectively treated using CAIRS. This framework is intended as an initial step toward more refined nomograms that incorporate additional parameters, such as prior cross-linking status, age, corneal biomechanics, and other factors that may emerge as relevant predictors of surgical outcomes.

This study reports significant improvements in visual acuity, refractive error, and corneal topography following femto-CAIRS in keratoconic eyes. Further development and standardisation of nomograms combined with industry-developed CAIRS profiles inbuilt into femtosecond lasers will likely increase the uptake and reproducibility of the procedure.

Acknowledgements

The Brisbane nomogram is based upon the work and kind advice of Doctors Soosan Jacob, Bader Khayat, Aylin Kilic, and Shady Awwad. We thank them for their generous support. Open access publishing facilitated by The University of Queensland, as part of the Wiley - The University of Queensland agreement via the Council of Australasian University Librarians.

Funding

The authors have nothing to report.

Conflicts of Interest

The authors declare no conflicts of interest.

Data Availability Statement

The data that support the findings of this study are available from the corresponding author upon reasonable request.

References

1. J. Colin, B. Cochener, G. Savary, and F. Malet, "Correcting Keratoconus With Intracorneal Rings," *Journal of Cataract and Refractive Surgery* 26, no. 8 (2000): 1117–1122, https://doi.org/10.1016/S0886-3350(00)00451-X.

2. J. I. Barraquer, "Basis of Refractive Keratoplasty—1967," *Refractive & Corneal Surgery* 5, no. 3 (1989): 179–193, https://doi.org/10.3928/1081-597X-19890501-13.

3. E. Coskunseven, G. D. Kymionis, N. S. Tsiklis, et al., "Complications of Intrastromal Corneal Ring Segment Implantation Using a Femtosecond Laser for Channel Creation: A Survey of 850 Eyes With Keratoconus," *Acta Ophthalmologica* 89, no. 1 (2011): 54–57, https://doi.org/10.1111/J.1755-3768.2009.01605.X.

4. A. Mounir, G. Radwan, M. M. Farouk, and E. M. Mostafa, "Femtosecond-Assisted Intracorneal Ring Segment Complications in Keratoconus: From Novelty to Expertise," *Clinical Ophthalmology* 12 (2018): 957–964, https://doi.org/10.2147/OPTH.S166538.

5. F. D'Oria, S. A. Bagaglia, J. L. del Alio Barrio, G. Alessio, J. L. Alio, and C. Mazzotta, "Refractive Surgical Correction and Treatment of Keratoconus," *Survey of Ophthalmology* 69, no. 1 (2024): 122–139, https://doi.org/10.1016/J.SURVOPHTHAL.2023.09.005.

6. M. J. Bautista-Llamas, M. C. Sánchez-González, I. López-Izquierdo, et al., "Complications and Explantation Reasons in Intracorneal Ring Segments (ICRs) Implantation: A Systematic Review," *Journal of Refractive Surgery* 35, no. 11 (2019): 740–751, https://doi.org/10.3928/1081597X-20191010-02.

7. J. Alio, S. Shah, C. Barraquer, K. Bilgihan, M. Anwar, and G. R. J. Melles, "New Techniques in Lamellar Keratoplasty," *Current Opinion in Ophthalmology* 13, no. 4 (2002): 224–229, accessed November 9, 2025, https://journals.lww.com/co-ophthalmology/fulltext/2002/08000/new_techniques_in_lamellar_keratoplasty.6.aspx.

8. K. Bilgihan, S. C. Özdek, A. Sari, and B. Hasanreisoglu, "Microkeratome-Assisted Lamellar Keratoplasty for Keratoconus: Stromal Sandwich," *Journal of Cataract and Refractive Surgery* 29, no. 7 (2003): 1267–1272, https://doi.org/10.1016/S0886-3350(02)02055-2.

9. B. U. Tan, T. L. Purcell, L. F. Torres, and D. J. Schanzlin, "New Surgical Approaches to the Management of KERATOCONUS and Post-Lasik Ectasia," *Transactions of the American Ophthalmological Society* 104 (2006): 212 accessed November 9, 2025, https://pmc.ncbi.nlm.nih.gov/articles/PMC1809910/.

10. S. Jacob, S. R. Patel, A. Agarwal, A. Ramalingam, A. I. Saijimol, and J. Michael Raj, "Corneal Allogenic Intrastromal Ring Segments (CAIRS) Combined With Corneal Cross-Linking for Keratoconus," *Journal of Refractive Surgery* 34, no. 5 (2018): 296–303, https://doi.org/10.3928/1081597X-20180223-01.

11. S. A. Nacaroglu, E. C. Yesilkaya, F. F. N. K. Perk, C. Tanriverdi, S. Taneri, and A. Kilic, "Efficacy and Safety of Intracorneal Allogenic Ring Segment Implantation in Keratoconus: 1-Year Results," *Eye* 37, no. 18 (2023): 3807–3812, https://doi.org/10.1038/s41433-023-02618-5.

12. S. Haciagaoglu, C. Tanriverdi, F. F. N. Keskin, K. D. Tran, and A. Kilic, "Allograft Corneal Ring Segment for Keratoconus Management: Istanbul Nomogram Clinical Results," *European Journal of Ophthalmology* 33, no. 2 (2023): 689–696, https://doi.org/10.1177/11206721221142995.

13. Y. Bteich, J. F. Assaf, A. A. Mrad, S. Jacob, F. Hafezi, and S. T. Awwad, "Corneal Allogenic Intrastromal Ring Segments (CAIRS) for Corneal Ectasia: A Comprehensive Segmental Tomography Evaluation," *Journal of Refractive Surgery* 39, no. 11 (2023): 767–776, https://doi.org/10.3928/1081597X-20231011-01.

14. N. Mechleb, D. Gatinel, L. Fitoussi, and A. Saad, "Six-Month Results of Multiple Femtosecond Laser-Assisted Corneal Allogeneic Ring Segments Implantation: A Case Series," *Cornea* 45, no. 3 (2026): 282–287, https://doi.org/10.1097/ICO.0000000000003831.

15. N. Mechleb, R. Flamant, C. Panthier, et al., "Technique of Corneal Allogenic Ring Segment Preparation Using Femtosecond Laser:

Preclinical Study on Human Corneal Grafts," *Journal of Cataract and Refractive Surgery* 50, no. 5 (2024): 518–522, https://doi.org/10.1097/J.JCRS.0000000000001399.

16. Y. Bteich, J. F. Assaf, F. Mul ̈ler, et al., "Femtosecond Laser-Assisted Graft Preparation and Implantation of Corneal Allogeneic Intrastromal Ring Segments for Corneal Ectasia: 1-Year Results," *Cornea* 44, no. 3 (2025): 360–367, https://doi.org/10.1097/ICO.0000000000003751.

17. Y. Bteich, J. F. Assaf, J. E. Gendy, et al., "Asymmetric All-Femtosecond Laser-Cut Corneal Allogenic Intrastromal Ring Segments," *Journal of Refractive Surgery* 39, no. 12 (2023): 856–862, https://doi.org/10.3928/1081597X-20231018-04.

18. J. H. Krumeich, J. Daniel, and A. Knalle, "Live-Epikeratophakia for Keratoconus," *Journal of Cataract and Refractive Surgery* 24, no. 4 (1998): 456–463, https://doi.org/10.1016/S0886-3350(98)80284-8.

19. B. Cronin, A. Ghosh, and C. Y. Chang, "Oxygen-Supplemented Transepithelial-Accelerated Corneal Crosslinking With Pulsed Irradiation for Progressive Keratoconus: 1 Year Outcomes," *Journal of Cataract and Refractive Surgery* 48, no. 10 (2022): 1175–1182, https://doi.org/10.1097/J.JCRS.0000000000000952.

20. G. S. Ying, M. G. Maguire, R. Glynn, and B. Rosner, "Tutorial on Biostatistics: Statistical Analysis for Correlated Binary Eye Data," *Ophthalmic Epidemiology* 25, no. 1 (2018): 1–12, https://doi.org/10.1080/09286586.2017.1320413.

21. G. S. Ying, M. G. Maguire, R. J. Glynn, and B. Rosner, "Tutorial on Biostatistics: Longitudinal Analysis of Correlated Continuous Eye Data," *Ophthalmic Epidemiology* 28, no. 1 (2021): 3–20, https://doi.org/10.1080/09286586.2020.1786590.

22. J. S. Parker, P. W. Dockery, and J. S. Parker, "Flattening the Curve: Manual Method for Corneal Allogenic Intrastromal Ring Segment Implantation," *Journal of Cataract and Refractive Surgery* 47, no. 11 (2021): E31–E33, https://doi.org/10.1097/J.JCRS.0000000000000555.

23. S. Mahler, A. Einan-Lifshitz, A. Shemer, A. Belkin, E. Pras, and B. Dubinsky-Pertzov, "Reproducibility of Manifest Refraction in Patients With Keratoconus Compared With Healthy Subjects: A Prospective Cohort Study," *American Journal of Ophthalmology* 266 (2024): 1–9, https://doi.org/10.1016/J.AJO.2024.04.023.

24. S. Jacob, A. Agarwal, S. T. Awwad, C. Mazzotta, P. Parashar, and S. Jambulingam, "Customized Corneal Allogenic Intrastromal Ring Segments (CAIRS) for Keratoconus With Decentered Asymmetric Cone," *Indian Journal of Ophthalmology* 71, no. 12 (2023): 3723–3729, https://doi.org/10.4103/IJO.IJO_1988_23.

25. A. Khanthik, N. Kasetsuwan, S. Yaisawang, U. Reinprayoon, V. Puangsricharern, and V. Satitpitakul, "Factors Predicting the Visual Outcome of Intracorneal Ring Segment for Keratoconus," *PLoS One* 19, no. 2 February (2024): 1–13, https://doi.org/10.1371/JOURNAL.PONE.0288181.

26. N. B. Bilen, I. F. Hepsen, and C. G. Arce, "Correlation Between Visual Function and Refractive, Topographic, Pachymetric and Aberrometric Data in Eyes With Keratoconus," *International Journal of Ophthalmology* 9, no. 8 (2016): 1127, https://doi.org/10.18240/IJO.2016.08.07.

27. B. Yucekul, C. Tanriverdi, S. Taneri, F. F. N. K. Perk, Y. Karaca, and A. Kilic, "Effect of Corneal Allogenic Intrastromal Ring Segment (CAIRS) Implantation Surgery in Patients With Keratoconus According to Prior Corneal Cross-Linking Status," *Journal of Refractive Surgery* 40, no. 6 (2024): e392–e397, https://doi.org/10.3928/1081597X-20240501-01.

28. A. J. Kanellopoulos, "Ten-Year Outcomes of Progressive Keratoconus Management With the Athens Protocol (Topography-Guided Partial-Refraction PRK Combined With CXL)," *Journal of Refractive Surgery* 35, no. 8 (2019): 478–483, https://doi.org/10.3928/1081597X-20190627-01.

29. W. A. Abou Samra, D. S. El Emam, R. K. Farag, and H. Y. Abouelkheir, "Simultaneous Versus Sequential Accelerated Corneal Collagen Cross-Linking and Wave Front Guided PRK for Treatment of Keratoconus: Objective and Subjective Evaluation," *Journal of Ophthalmology* 2016, no. 1 (2016): 2927546, https://doi.org/10.1155/2016/2927546.

30. X. Chen, A. Stojanovic, Y. Xu, et al., "Medium-To Long-Term Results of Corneal Cross-Linking for Keratoconus Using Phototherapeutic Keratectomy for Epithelial Removal and Partial Stromal Ablation," *Journal of Refractive Surgery* 33, no. 7 (2017): 488–495, https://doi.org/10.3928/1081597X-20170504-03.

31. M. S. Shaheen, A. Shalaby Bardan, D. P. Piñero, et al., "Wave Front-Guided Photorefractive Keratectomy Using a High-Resolution Aberrometer After Corneal Collagen Cross-Linking in Keratoconus," *Cornea* 35, no. 7 (2016): 946–953, https://doi.org/10.1097/ICO.0000000000000888.

32. J. J. Males and D. Viswanathan, "Comparative Study of Long-Term Outcomes of Accelerated and Conventional Collagen Crosslinking for Progressive Keratoconus," *Eye* 32, no. 1 (2018): 32–38, https://doi.org/10.1038/eye.2017.296.

Supporting Information

Additional supporting information can be found online in the Supporting Information section. **Data S1:** Supporting Information.